



ARTICLE

Transformation of MRI Images to Three-Level Color Spaces for Brain Tumor Classification Using Deep-Net

Fadl Dahan*

Department of Management Information Systems, College of Business Administration-Hawtat Bani Tamim,
Prince Sattam bin Abdulaziz University, Al-Kharj, 11942, Saudi Arabia

*Corresponding Author: Fadl Dahan. Email: f.naji@psau.edu.sa

Received: 22 November 2023 Accepted: 27 February 2024

ABSTRACT

In the domain of medical imaging, the accurate detection and classification of brain tumors is very important. This study introduces an advanced method for identifying camouflaged brain tumors within images. Our proposed model consists of three steps: Feature extraction, feature fusion, and then classification. The core of this model revolves around a feature extraction framework that combines color-transformed images with deep learning techniques, using the ResNet50 Convolutional Neural Network (CNN) architecture. So the focus is to extract robust feature from MRI images, particularly emphasizing weighted average features extracted from the first convolutional layer renowned for their discriminative power. To enhance model robustness, we introduced a novel feature fusion technique based on the Marine Predator Algorithm (MPA), inspired by the hunting behavior of marine predators and has shown promise in optimizing complex problems. The proposed methodology can accurately classify and detect brain tumors in camouflage images by combining the power of color transformations, deep learning, and feature fusion via MPA, and achieved an accuracy of 98.72% on a more complex dataset surpassing the existing state-of-the-art methods, highlighting the effectiveness of the proposed model. The importance of this research is in its potential to advance the field of medical image analysis, particularly in brain tumor diagnosis, where diagnoses early, and accurate classification are critical for improved patient results.

KEYWORDS

Camouflage brain tumor; image classification; weighted convolutional features; CNN ResNet50

1 Introduction

The human brain is like the control center for the human body. It takes information from our senses, processes it, and tells human muscles what to do. Abnormal growth of brain cells called brain tumors, can be a serious problem. Additionally, the World Health Organization (WHO) has categorized brain tumors (BTs) into four groups (Grades I–IV) based on how severe they are [1]. In the field of medical science, there has been a lot of development in several imaging techniques to aid in the diagnosis of diseases. These include X-rays, ultrasound, PET scans, CT scans, MRS, SPECT scans, and MRI [2]. These imaging technologies provide valuable insights for doctors to examine different parts of the human body, ensuring the diagnosis and treatment of various diseases. Among these, MRI stands out as the preferred and most valuable method because it shows images with high resolution



and provides accurate details about the structure of the body. It is especially effective in capturing many types of brain tumors like Glioma, Pituitary tumors, and Meningioma [3]. Fig. 1 shows the brain tumor types. In fact, MRI is widely regarded as one of the most reliable and widely used tools for classifying brain tumors. Grade III and Grade IV BTs are especially fast-growing tumors and can spread to other parts of the body, harming different healthy cells. Detecting and identifying BTs early is crucial because it helps doctors to plan the right treatment, using tools like MRI and other images [4].

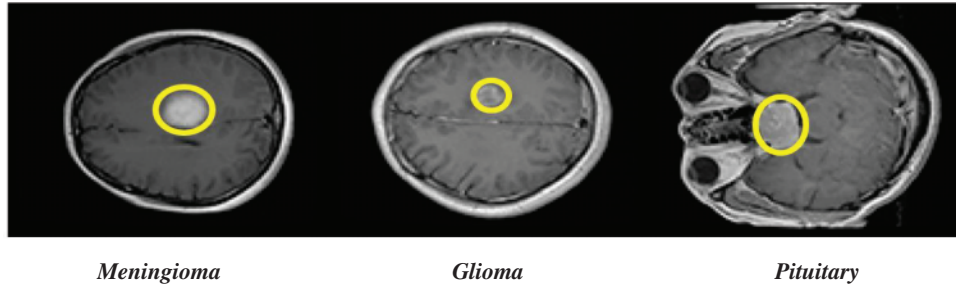


Figure 1: Axial view of Glioma, Pituitary brain tumors, and Meningioma types

There are three types of primary brain tumors: Glioma, Pituitary tumors, and Meningioma. Pituitary tumors are generally non-cancerous that grow in pituitary glands, which produce vital hormones in the body [5]. Gliomas develop from specific brain cells called glial cells [6]. Meningioma tumors usually grow on the protective and outer membrane that covers the spinal cord and brain [7]. Identifying the difference between normal brain tissue and abnormal tissue is vital when looking for BTs. Due to differences in size, shape, and location, detecting BTs can be challenging and still an ongoing problem to be addressed. The field of medical images processing plays an important role for BT analysis, including tasks like classification, segmentation, and detection [8,9]. The accurate classification of brain tumor is necessary to diagnose the tumor type timely if it exists. Modern diagnosis systems aided by computer in biomedical image processing to help radiologists in guiding patients and improve BT classification [10,11]. For brain tumor categorization, the use of advanced and pre-trained CNN models has made great progress, allowing researchers to make speedy and accurate decisions. Due to the complexity of data, categorizing brain images with high accuracy remains a difficult challenge. Using publicly available datasets, this study aims to develop a completely automatic CNN model that performs color transformation and selects optimized features for identifying brain tumors into different categories.

The motivation for this research to study hidden brain tumors in image datasets stems from this important goal and to enhance the early detection and diagnosis of these tumors. Accurate identification of brain tumors is a challenging due to their subtle and complex pattern. By focusing on camouflaged tumors within image datasets, researchers are dedicated to develop advanced image processing and machine learning algorithms, the aim is to enhance the detection and classification of these hidden tumors with high precision and efficiency. Early detection can significantly improve patient outcomes by assisting timely medical interventions and treatment strategies, eventually lead to improve prognosis and an enhanced quality of life for individuals dealing with this condition. Color transformation plays an important role by enhancing the visual representation of grayscale images, assisting in the accurate interpretation and analysis of tumor patterns and structures. Our proposed methodology outperforms in the existing deep learning approaches in terms of classification accuracy, even with reduce amount of training data, as described in the confusion matrix.

The proposed approach for classifying BT consists of three steps: Improving contrast, transforming images into color spaces, fusing multiple feature fusion, and feature selection for final classification. The following are the important contributions of this approach:

- A novel technique known as MRI image modification is introduced to improve the contrast in MRI brain tumor pictures, aiming to improve the internal contrast of the robust feature selection for brain tumor camouflage.
- The ResNet50 model is applied for feature extraction, focusing on the weighted features of the first convolutional layer through three distinct color transformations. These features are joined using a sequential canonical correlation-based technique.
- The Marine Predator Algorithm (MPA) is used to select features and employ diverse machine learning based classifiers with different learning rate and cross validation techniques.

2 Literature Review

Many techniques have been introduced over time to classify and segmentation of BT data. While more modern methods have made use of deep learning models [12], some of these techniques still rely on conventional machine learning. We focus on BT classification research in this section.

There are several methods that have been proposed, incorporating transfer learning on custom dataset, deep CNN features extraction and classification, and deep ensemble methods to achieve better accuracy. In [13], authors introduced a neural network and segmentation base framework that automatically detects tumors in brain MRI images. To evaluate feature extraction from an MRI brain image, the methodology extended PCA and different classifiers are used for feature classification. The average rate of recognition is 88.2%, and a peak rate of 96.7%. Tazin et al. [14] defined a model aimed at increasing accuracy by transfer learning techniques. They applied three different techniques that used pre-trained CNN models and obtained accuracy rates of 88.22% using VGG19, 91% using Inception V3, and 92% using Mobile Net V2, respectively. In comparison to the other models, the authors found that MobilnetV2 is far more useful. In [15], Abd-Ellah et al. presented a PDCNN framework to identify and categorizing gliomas in MRI images. Dataset (The braTS-2017) employed to evaluate the proposed PDCNNs. The study uses 1200 photographs in the PDCNN training phase, 150 images in the PDCNN for validity purpose, and 450 images are in the PDCNN test phase. This framework produced 97.44% accuracy, 97.0% sensitivity, and 98.0% specificity. Afshar et al. [16] proposed using capsule networks to serve as a CNN topology with a precision of 90.89%, the proposed technique employs the Figshare dataset to focus on the major location of tumors and their relationships to nearby tissues. In [17], Nazir et al. proposed a model using the ANN technique. Groups of two malignancies have been targeted in their proposed research: Beginning stage tumors and malignant tumors. In the first stage, images are preprocessed with filters then the average color moment approach is used to extract features. After characteristic mappings to the ANN classification accuracy is 91.8%. In [18], Luyan et al. developed a system that is capable of extracting outcomes from the connectome of a complex human brain by expanded network analysis strategies. As a result, they used a multistage feature selection technique to select those features that lessens the feature redundancy. Hence, they used a support vector machine (SVM) to generalize the outcomes of HGG, the result was not respectable and moral. Finally, their approach attained an accuracy of 75%. Sawant et al. [19] devised a strategy that highlights the tensor flow procedure to detect brain tumors using MRI. 5-layer CNN model implemented using tensor flow. A total of 1800 MRIs were used on the dataset, with 900 of them being tumors and the other 900 being non-tumorous. Among 35 epochs, training accuracy was 99% and validation accuracy was 98.6%.

Researchers used many model based and features selection-based methods. In [20], Soesanti et al. suggested a model using the statistical histogram equalization technique, that applies a transformation to each and every pixel by the calculation of multiple statistical parameters like variance, entropy, etc. This model is used to define low and high-level images of cervical glioma. The idea is to achieve an accuracy level of 83.6%, a sensitivity rate of 80.88%, and 86.84% of specificity. In [21], the authors used the features of a pre-trained model and employed a genetic algorithm for feature selection. This novel method produced outstanding results, achieving an astounding 95% accuracy on two challenging datasets, BRATS2018 and BRATS2019. Attique et al. [22] also used a multimodal approach to classify BT images where, for features extraction used VGG16 and VGG19. In addition, the authors achieved 95.2% results on the BraTs2018 dataset. In a similar work proposed in [23], the author extracted deep features for the segmenting, localization, and classifying of brain tumors, achieving the best accuracy of 95.71% on the selected brain tumor dataset. Francisco et al. [24] introduced deep CNN based BT segmentation and classification on the T1-CE MRI images dataset for multi-class type tumor classification and the authors got good accuracy on the selected dataset. In [25], Çinar et al. developed a hybrid strategy for brain tumor identification in which the tumor was identified from MRI using deep learning algorithms. CNN model was employed to predict eight additional layers and remove the last five layers from ResNet50. As a result, their created model outperformed than other deep learning models by 97.2%. In [26], Anil et al. proposed a technique, which includes a network of classification algorithms that divides the MRI images into two categories: Those with tumors and those without. The classification system was retrained to identify brain tumors using the technique of transfer learning. According to the results, VGG19 was really effective, accuracy of percentage of 95.78%.

3 Proposed Methodology

In this section, a novel and comprehensive model is presented for MRI image transformation into vibrant color. A pre-trained CNN model ResNet50 is employed to extract deep features from grayscale MRI images, which are then fused, selected, and classified. The overall proposed model of MRI image transformation is presented in Fig. 2.

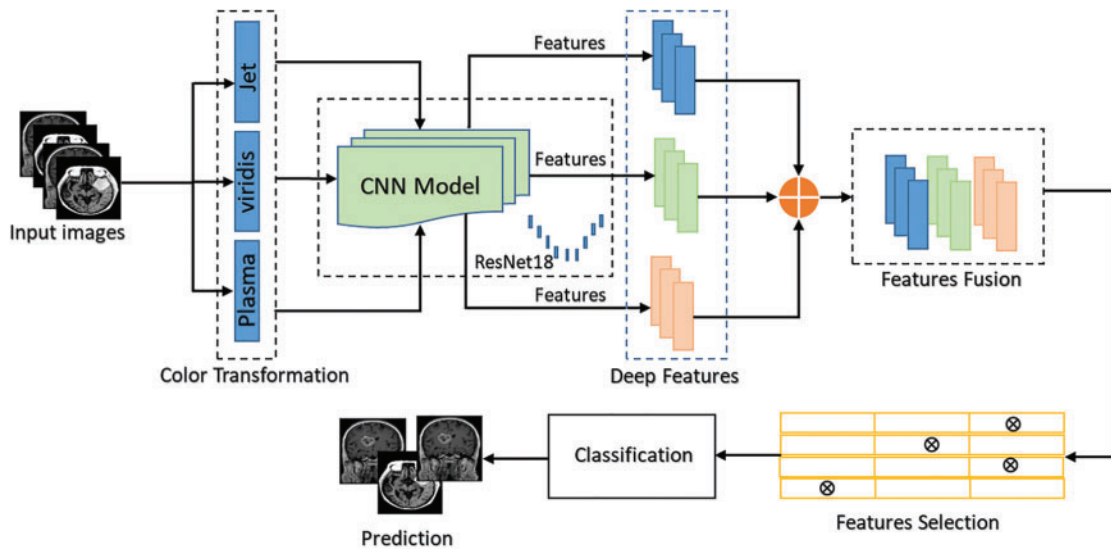


Figure 2: Proposed system diagram

The models specify brain tumor classification and support on unique imaging features may bound its applicability to varied disorders with diverse indicators as well as can to detect camouflaged brain tumors. Acquiring diverse and illustrative training data for numerous conditions is crucial but may be challenging, possibly affecting the model's performance. The resource-intensive nature of profound neural networks, probable issues with toughness and transfer learning, and obedience to regulatory standards further underline the complications involved in ranging the model beyond its original focus on brain tumors. Addressing these challenges requires a thoughtful approach, including proven authentication, association with domain professionals, and reflection of monitoring compliance to confirm the model's responsibility and operating application across various medical imaging situations.

This proposed model has been carefully tested in three main steps. First, grayscale images are converted into color images after that color MRI images are transformed into: Plasma, Viridis, and Jet. To extract strong visual features from each category a pre-trained CNN model is used. In the second step, these features are then fused together in a single feature vector which selectively holds the most relevant information. Feature selection is applied to classify MRI images. This procedure results in successful MRI image categorization, resulting in findings that are both informative and visually appealing. The following sections provide a detailed description of various modules.

3.1 Preprocessing

In the preprocessing step, grayscale MRI images are resized to enhance further colorization while improving the model's reliability and adaptability. To reduce the resolution of the MRI images, the most common approach is to scale them to a rectangular format with appropriate dimensions. In this proposed work 224×224 size input images are used to train our model. After resizing the image, the next step is to remove the noise.

Noise removal in brain MRI images is typically advantageous as it enhances the picture quality, making the images easier to read and assisting inaccurate diagnosis. In this proposed work Gaussian filter is used for noise reduction. The Gaussian filtration is defined as follows:

$$G(a_o, i_0) = \frac{1}{2\pi\sigma^2} - \frac{(a_o^2 + i_0^2)}{2\sigma^2} \quad (1)$$

where $G(a_o, i_0)$ is the Gaussian function at coordinates (x, y) and σ represents the value of standard deviation in Gaussian distribution.

After removing the noise from MRI images normalization is the next and an important step before color transformation. The next step is normalization MRI images, as grayscale images are going to be converted into colorized images. The procedure starts with selecting grayscale MRI images and learning about their pixel value range, which typically ranges from 0 to 255. A linear scaling process is used to normalize these grayscale images, which typically rescales the pixel to [0, 1] or [-1, 1]. This rescaling creates a strong base for further color transformation. Differences in pixel value scales do not affect color transformation and generate visually appealing colorized MRI images. To calculate the range from [0, 1] normalization is applied as:

$$I_{normalize} = \frac{x - x_{min}}{x_{max} - x_{min}} \quad (2)$$

To calculate the range from [-1, 1] normalization is applied as:

$$I_{normalize} = \frac{2 * (x - x_{min})}{(x_{max} - x_{min}) * -1} \quad (3)$$

where $I_{normalize}$ is the new value, x_{min} is the minimum pixel value and x_{max} maximum pixel value. After normalization, all grey scale pixels are normalized within a specified range which is more suitable for color transformation.

3.2 Color Transformation

Color transformation is the process of transforming grayscale images into visually appealing color images. In this proposed work colorization process is a fundamental step. In the first step, normalized greyscale images are transformed into colored images to enhance visual understanding and diagnostic accuracy. The MRI image of the human brain is extremely complex, with several structures and types of tissue that can be difficult to detect in grayscale. Different anatomical spots or pathologies and abnormalities become more visibly apparent when color is introduced. In the medical field, the majority of grayscale images require colorization to help the doctor for detailed understanding. We convert $I_{normalize}$ MRI images into colored images by this equation:

$$I_{color} = Concat(I_{normalized} + I_{normalized} + I_{normalized}) \quad (4)$$

In the second step, colored MRI images are then transformed into three color spaces: Plasma, Viridis, and Jet. These color spaces highlight different features of the MRI images and enhance visual aspects of the image which can fulfill the diagnostic and analytical needs. Plasma, Viridis, and Jet all highlight different features, such as structural features, and tissue contrast. The Plasma color spaces are made up of gradients, and their transformation can be expressed by this equation:

$$I_{plasma} = (0.1717 * G) + (0.757 * B) - (0.1882 * G * B) \quad (5)$$

In this equation, to find the color space of plasma Green (G) and Blue (B) components are used in this calculation. The coefficients 0.1717, 0.757, and 0.1882 determine the contribution of G and B to Plasma color space. To find the Viridis, the equation which is used as follows:

$$I_{viridis} = (0.1696 * G) - (0.3544 * R) + (0.5679 * B) \quad (6)$$

In this equation, the coefficients 0.1696, 0.3544, and 0.5679 are used to determine Viridis color spaces and are also calculated by Red (R) and Blue (B) components. For Jet color space, the equation is used as follows:

$$I_{jet} = (0.3016 * R) + (0.1979 * G) - (0.4287 * B) \quad (7)$$

The contributions of R, G, and B to find the jet color space are determined by the coefficients 0.3016, 0.1979, and 0.4287. After the transformation of colored images into Plasma, Viridis, and Jet as depicted in [Fig. 3](#), the next step is to extract features from these transformed images.

The primary objective of color transformation is to identify the essential features for achieving precise classification outcomes. In addition, the visual illustration of the data can influence the capability to distinguish among different configurations or tissues in the MRI. This differentiation is vital for precise classification. Certain color maps may high spot image artifacts contrarily. Finding and understanding artifacts is essential for preprocessing steps and improving the strength of classification models. Though the color map choice is vital for visualization and understanding, it is just one feature of the overall heterogeneity data analysis. Moreover, the accuracy of classification is usually influenced by the features extracted from the data, the choice of the classification algorithm, and the quality of the training data, between other features. Consequently, the development in classification accuracy, if any, would expected to be a result of a more contemporary analysis and interpretation simplified

by the use of suitable color maps. It might see which one provides the most efficient illustration for distinguishing related features in provided MRI data by testing with different color maps.

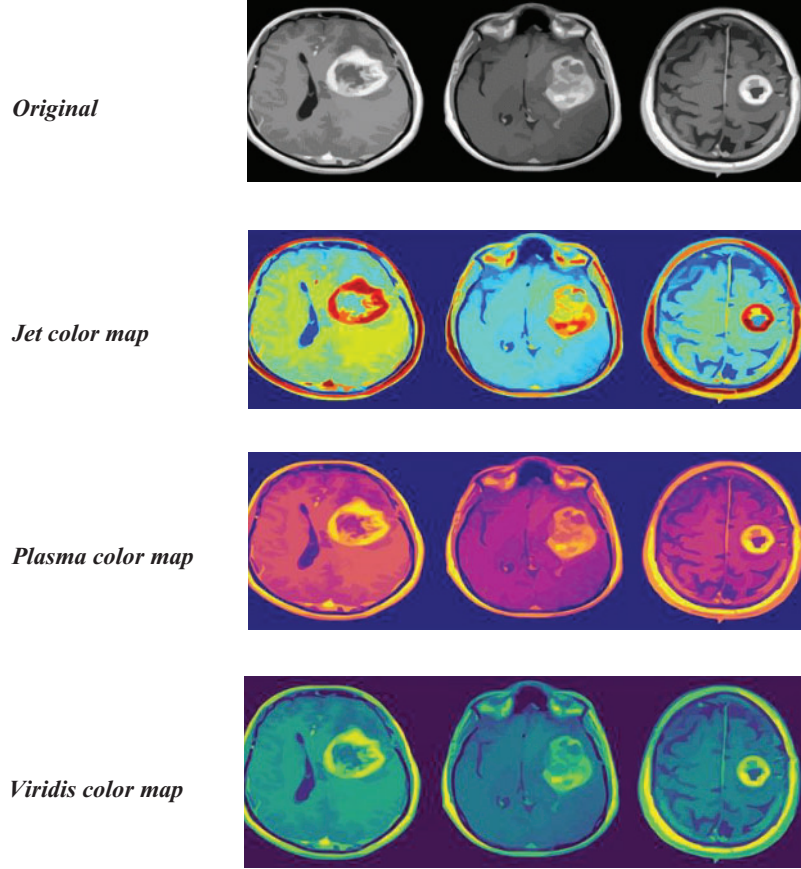


Figure 3: Transformation Plasma, Viridis, and Jet of sample images

3.3 Transfer Learning

In computer vision transfer learning Tl is commonly represented by utilizing pre-trained models. Models that have been trained before can be employed due to the high computational expense of training such models from scratch. In transfer learning, define feature vector $fv = \{v_{plasma}, v_{viridis}, v_{jet}\}$ and probability distribution as $X = \{fv, P(fv)\}$. In which ground truth $G = \{j1, j2, \dots, jn\}$ and objective function $O = \{G, L(x)\}$, whereas $L(x)$ is an unknown label class. $P(j|x)$ is a probabilistic function. T_l and l_{rate} represent transfer learning and learning rate, respectively. $(I(Tf))$ represents the targeted function, while Tf represents the targeted output. The main objective of transfer learning in this proposed study is to improve the learning rate to predict the targeted object by using the recognition function ($L(x)$) based on the training learned from Tl and Tf where $Tl \neq Tf$ and $l_{rate} \neq Tf$.

3.3.1 Feature Extraction and Fusion Using Pre-Trained ResNet50

For deep feature extraction, a pre-trained CNN model ResNet50 is employed because it is an advanced feature extractor, completing a sequence of computations, this model generates in detailed feature maps. This model selection is for its great resilience and effectiveness in biological data analysis applications. The goal of using this model is to analyze images of various sizes and obtain depth

characteristics. To finish this procedure, we first extend the 32×32 image to $224 \times 224 \times 3$. As input for pre-trained models, we transform I_{color} into a three-color space I_{plasma} , $I_{viridis}$, I_{jet} . These color maps enable better visual representations of brain structures and give a multidimensional perspective of the MRI images, boosting the interpretability of the model to grasp subtleties.

This approach recognizes the diverse information provided by each color map category and uncovers unique visual information that is related to each category during its scanning process. Jet may highlight certain structures, Viridis could emphasize many others, and Plasma may expose still another aspect, resulting in an array of feature vectors F_v . The training process on image is performed by using DCNN pre-trained models to get features via the FC7 layer. We use Global Average Pooling (GAP) to combine these maps and transform them into feature vectors for each category. The global average pool is referred to as F_{plasma} , $F_{viridis}$, and F_{jet} , respectively.

The combination of features from three color spaces is used to conduct feature fusion. The fusion of these three is carried out as follows:

$$F_{us} = [F_{jet} F_{viridis} F_{plasma}] \quad (8)$$

As a result, the concatenation process increases feature diversity, allowing the classifier to perform better. Subsequently, these characteristics are fused and concatenated to get deep features from this proposed model.

3.4 Feature Selection

Feature selection is the most important phase in the study and it is critical for improving the model's efficiency and interpretability. A significant F_v is obtained after feature extraction from the three-color spaces (Jet, Viridis, and Plasma). After feature extraction, high dimensionalities may be encountered. This dimensionality reduction is done with care because it finds a balance between computing efficiency and the retention of important information inside the MRI images. Reducing the number of features reduces execution time while increasing performance. The outcome of feature selection is a single feature vector that provides data for subsequent classification tasks which improves the overall accuracy. The Marine Predator Algorithm (MPA) is used to select features; it is a nature-inspired algorithm.

The Marine Predator Algorithm (MPA) influences bio-inspired principles, pretending predatory crescendos of marine types. Over mathematical formulation, population initialization, and obliging hunting, MPA competently explores way out spaces for optimization difficulties. Predators dynamically adjust positions using movement and enclosing strategies, causative to solution convergence. Fine-tuning constraints, describing convergence criteria, and speaking algorithmic complexity make sure practical applicability. MPA's achievement lied in its simulation of marine performances, offering an adaptive and effective optimization methodology with broad applications in varied domains, from engineering to artificial intelligence.

In MPA by combining exploration and exploitation methods, predators update their position. A simplified predator position update equation is:

$$p_i^a = p_i^{a-1} + \Delta p_i^a \quad (9)$$

In this equation, i is the initial position and a is the attempt p_i^{a-1} shows the previous position of the predator, Δp_i^a shows the change in location as a result of hunting and foraging techniques. The next step is fitness evaluation using the objective function $f(t)$, where t denotes the predator's current position.

$$F_{fitness}(p_i^a) = f(p_i^a) \quad (10)$$

After fitness evaluation, the next step is to find the best-optimized solution. A basic formula for finding the best-optimized solution is:

$$p_i^{a+1} = BestSelect(p_i^a, p_j^a, \dots, p_n^a) \quad (11)$$

where *BestSelect* is a feature selection process used to select the best-optimized features, then selected features are classified using some highly effective classification classifiers. These classifiers are super-smart, and we employ them to determine which group each colored image belongs to. We use performance metrics to evaluate how accurate our model is and to what extent it is good at detecting the appropriate tumors in colored MRI images. We can also calculate accuracy, precision, and recall ensuring our model's correctness with different classifiers.

4 Result and Experimental Setup

To conduct experiments, this study utilized a dataset consisting of 7023 BT images collected from three different sources: Figshare [27], SARTAJ and Br35H described in [28] collected was downloaded from the Kaggle compiled by Masoud [29]. These images were categorized into four distinct classes, encompassing both normal brain images and three specific types of brain tumors, namely Glioma, Meningioma, and Pituitary tumors. Moreover, the proposed integrated brain tumor classification system was implemented using MATLAB 2022b on a computer with an Intel Core i7 processor, 16 GB of RAM, and an 8 GB graphics card. A series of different experiments are performed to evaluate the proposed model.

In the initial experiment as shown in Table 1, the primary objective was to evaluate the classification model's accuracy in the context of brain tumor classification. For this experiment we utilize the ResNet50 architecture, a powerful and established deep learning model. The core focus of the experiment was to evaluate the model's ability to accurately classify brain tumor images across various color transformations.

Table 1: Accuracy and area under the curve on all SVM of different transform color features results

Classification	Plasma		Viridis		Jet	
	AUC (%)	ACC (%)	AUC (%)	ACC (%)	AUC (%)	ACC (%)
Liner	98.75%	91.7%	98%	91.1%	98.75%	91.8%
Quadratic	99.25%	94.2%	99%	93.4%	99.25%	93.9%
Cubic	99.25%	94.7%	99%	94.1%	99.25%	94.5%
Fine gaussian	89.0%	49.0%	89%	49.8%	87.75%	49.6%
Medium gaussian	98.75%	91.6%	99%	91.2%	99.0%	91.8%
Coarse gaussian	97.25%	87.6%	97%	86.9%	97.5%	87.4%

In this experiment as presented in Table 2 shows that, the test results for our model with four distinct classes as discussed above, notably achieved impressive precision rate for each category up to 98.12% for Glioma, 91.7% Meningioma, and so on. These precision scores provide insights into the accuracy of our classification for each class, ensuring robust performance and reliability in our model's predictions.

Table 2: Test precision values for each category of the proposed model on Cubic SVM

BT types/results	Training images	5-fold validation precision	10-fold validation precision	Testing images	Precision
Glioma	1321	96.1%	97.00%	300	98.12%
Meningioma	1339	90.2%	91.30%	306	91.70%
Pituitary	1457	95%	97.02%	300	98.20%
No-tumor	1595	96%	96.52%	405	98.02%

In the next experiment as presented in [Table 3](#), we harnessed the capabilities of well-established pre-trained models, including GoogleNet, ResNet18, and ResNet50, to extract discriminative features. Employing Support Vector Machines (SVM) for classification, we observed that Cubic SVM emerged as the top-performing classifier among the three models, GoogleNet, ResNet18, and ResNet50 and results are 95.5%, 95.2% and 98.4% achieved high accuracy, respectively. This approach demonstrated favorable results, underscoring the efficacy of utilizing Cubic SVM for accurate and effective classification. Cubic SVM performed well because functions as a non-linear classifier, enabling it to effectively represent intricate data relationships that might not be linearly distinguishable. Particularly in image classification, where decision boundaries can be intricate, a non-linear approach like Cubic SVM excels in capturing nuanced patterns that may elude a linear classifier.

Table 3: Pre-tainted CNN model features based experiments and accuracy on different all SVM classifiers on the proposed model

Classifier/features	GoogleNet	ResNet18	ResNet50
Medium gaussian	93.1%	93.4%	94.2%
Linear	91.7%	91.1%	94.1%
Quadratic	94.1%	93.9%	95.9%
Cubic	95.5%	95.2%	98.4%
Fine gaussian	49.7%	42.3%	44.9%
Coarse gaussian	88.4	88.7%	90.5%

[Fig. 4](#) shows the confusion matrix of Cubic SVM, that shows height results on the proposed model.

In [Table 4](#), the proposed brain tumor classification model has demonstrated superior performance with a Macro F1-Score of 96.44%, a Macro Recall of 96.37%, and a slightly higher Macro F1-Score of 96.51% on Cubic SVM. These metrics collectively signify its exceptional accuracy, reliability, and balanced classification capabilities. Notably, the model showcases strong recall, minimizing the risk of missing actual brain tumor cases. Its consistency is shown from closely aligned Macro F1-Scores, reinforcing its reliability across different evaluation metrics. Graphic representation is presented in [Fig. 5](#).

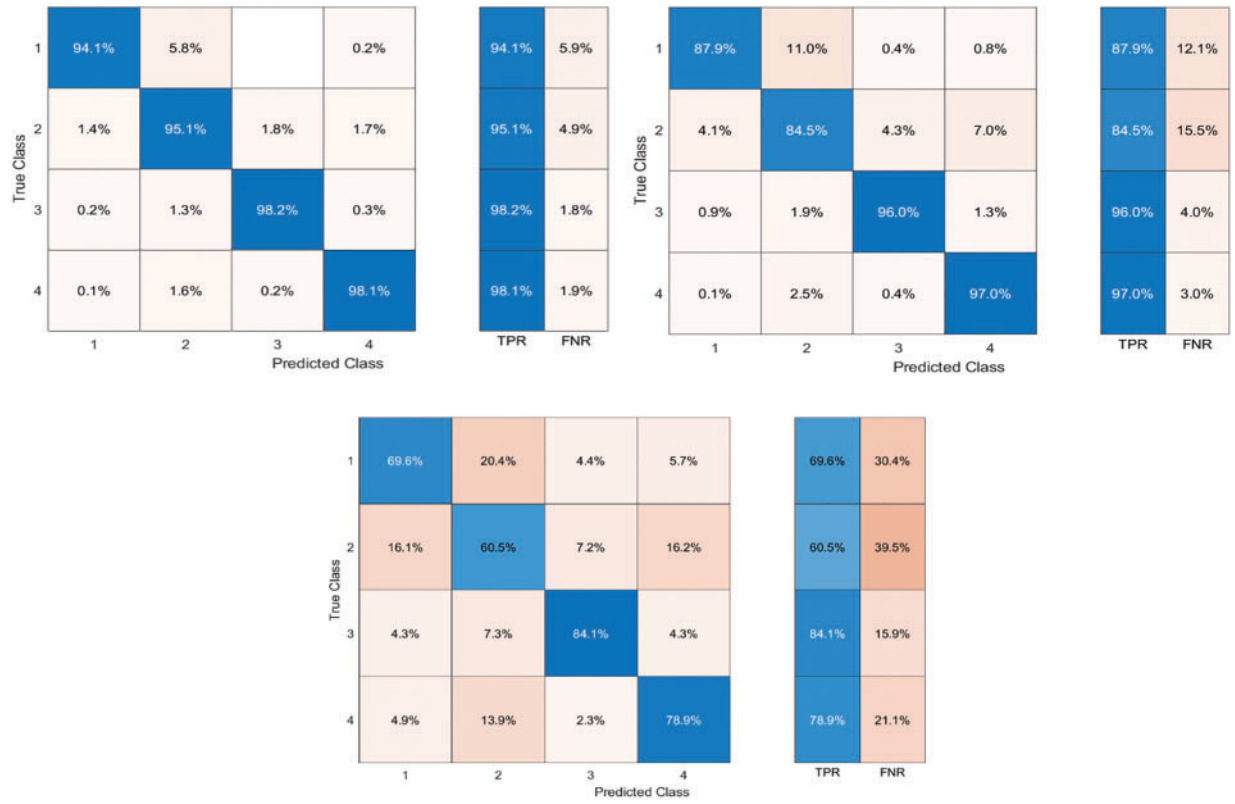


Figure 4: Confusion matrix of Cubic SVM as presented in [Table 2](#)

Table 4: Class-wise evaluation metrics on Cubic SVM

Tumor type	F1-Score	Recall	Precision
Glioma	96.00%	94.10%	98.12%
Meningioma	93.37%	95.2%	91.70%
Pituitary	98.24%	98.5%	98.20%
No-tumor	98.05%	98.1%	98.02%
Macro F1-Score	96.44%		
Macro recall	96.37%		
Macro precision	96.51%		

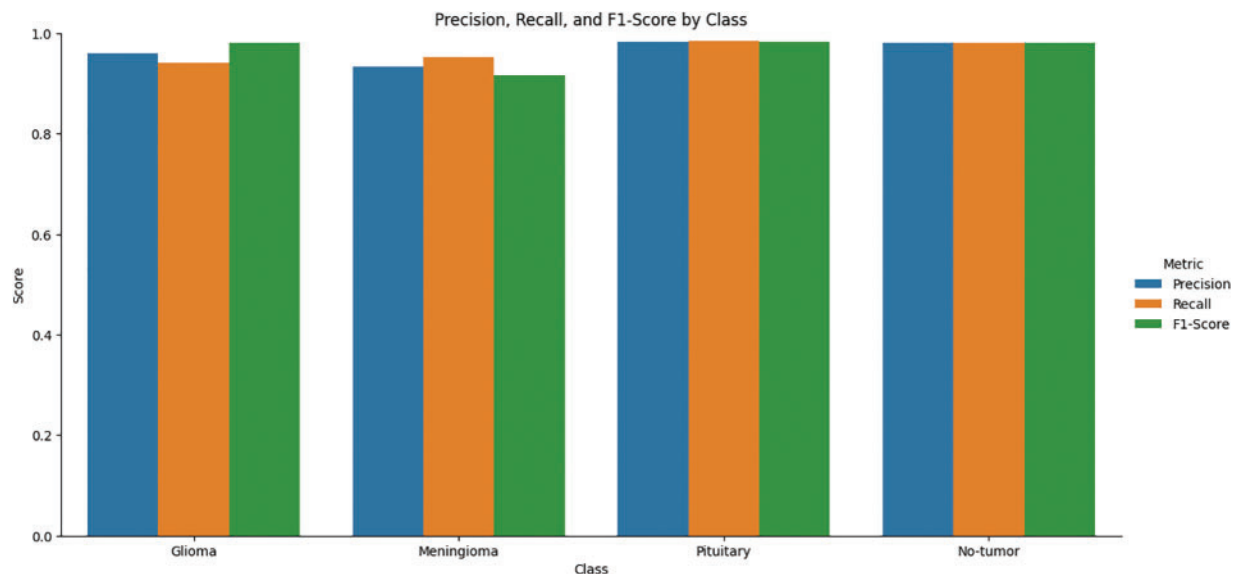


Figure 5: Graphical representation of class-wise evaluation metrics on Cubic SVM

Results are compared with existing state-of-the-art methods as presented in Table 5. The main focus of the experiment’s results discussion is the notable divergence from the standard methodology used by the majority of field authors. While many authors have traditionally depended on the publicly available dataset namely the ‘Figshare’ dataset for their research, consisting of a total of 3064 images, our experiment took a more comprehensive and forward-thinking approach. We combined three distinct datasets, namely ‘Figshare’, ‘SARTAJ’, and ‘Br35H’, totaling 7023 images. This bold step was motivated by the recognition of the increasingly complex nature of real-world datasets, which often extend beyond the confines of singular, controlled datasets. The decision to combine these datasets was validated by the remarkable results achieved during the experiment. By working with a more complex dataset, our model demonstrated significantly produced accuracy, particularly when challenged with the complex nature of the combined dataset. This approach showcased the model’s robustness and capacity to handle the details of real-world data, which often exhibit variations, nuances, and complexities that transcend the boundaries of individual datasets.

Table 5: Comparison results on existing work on publically available dataset

Ref.	Method	Classes type	Dataset	Accuracy
[30], 2019	Transfer learning of GoogleNet Features	Multi class 3064 brain MRI images	Figshare	98.00%
[31], 2022	Custom 23 layers CNN model	3064 brain MRI images	Figshare	97.80%
[32], 2020	GAN + ConvNet	3064 brain MRI images	Figshare	95.60%
[33], 2021	Custom Mask-RCNN	Multi + Binary class 3064 brain MRI images 253 MRI sample	Figshare and Kaggle (publically available dataset)	98.34%
[34], 2021	VGG19 + CNN	3064 brain MRI images	Figshare	98.54%

(Continued)

Table 5 (continued)

Ref.	Method	Classes type	Dataset	Accuracy
[35], 2023	Fine-tuned EfficientNetB2	3064 brain MRI images	Figshare	98.56%
Proposed	ResNet50 features Fusion Jet+ Viridis + Plasma	Multi class 7023 brain MRI images	Combined Figshare, SARTAJ, and Br35H (publically available dataset)	98.72%

The challenge of identifying camouflaged brain tumors, and the use of color transformation becomes a key solution for accurate classification. Color transformation represents the process of converting grayscale images into visually compelling color images, thereby enhancing the visibility of nuanced features, including those indicative of brain tumors. By incorporating color transformation techniques into the classification process, researchers aim to improve the diagnostic accuracy and effectiveness of tumor detection methodologies. By color transformation, grayscale images are infused with distinct hues and shades, empowers clinicians and machine learning algorithms to identify abnormal patterns and structures associated with brain tumors more effectively. Color transformation boosts the contrast and visibility of tumor-related abnormalities against the background tissue, aids the improving the classification accuracy and early detection. Integrating color transformation with classification algorithms provides healthcare professionals to navigate complex datasets, allows timely and well informed diagnostic decisions. By adopting synergistic approach not only improves the precision of tumor classification but also facilitate the treatment process, potentially leading to improved patient outcomes and prognosis. This depth of analysis not only enhances the scientific accuracy of the study but also facilitates meaningful interpretation and application of the findings. Therefore, the integration of color transformation techniques represents a promising direction for the improvement of brain tumor detection and classification, driving progress in medical imaging and diagnostic approaches.

5 Conclusion

In this study, we proposed a model based on color transformation which shows that the integration of color-transformed images with the progressive capabilities of deep learning, utilizing the ResNet50 architecture, has yielded significantly improved results. We conducted our experiments on a significantly more complex dataset than previous studies, and the proposed model demonstrated the ability to classify brain tumors with achieving an accuracy rate of 98.72%. This highlights the potential and effectiveness of this innovative approach, which combines state-of-the-art techniques to achieve superior results in the field of tumor classification. Data used in the article is publically available at: <https://www.kaggle.com/datasets/masoudnickparvar/brain-tumor-mri-dataset>.

Acknowledgement: The author extends his appreciation to Prince Sattam bin Abdulaziz University for funding this research work through the Project Number (PSAU/2023/01/24607).

Funding Statement: The research work received funding from Prince Sattam bin Abdulaziz University through the Project Number (PSAU/2023/01/24607).

Author Contributions: The authors confirm contribution to the paper as follows: Study conception, design data collection, analysis and interpretation of results, and draft manuscript preparation: F. Dahan. The author reviewed the results and approved the final version of the manuscript.

Availability of Data and Materials: The data used to support the findings of this study are available from the author upon request (f.naji@psau.edu.sa).

Conflicts of Interest: The author declares that he has no conflicts of interest to report regarding the present study.

References

- [1] N. A. Samee *et al.*, “Classification framework for medical diagnosis of brain tumor with an effective hybrid transfer learning model,” *Diagn.*, vol. 12, pp. 2541, 2022. doi: [10.3390/diagnostics12102541](https://doi.org/10.3390/diagnostics12102541)
- [2] S. R. Cherry, “Multimodality imaging: Beyond PET/CT and SPECT/CT,” in *Semin. in Nuclear Med.*, 2009, pp. 348–353.
- [3] M. Yildirim, E. Cengil, Y. Eroglu, and A. Cinar, “Detection and classification of glioma, meningioma, pituitary tumor, and normal in brain magnetic resonance imaging using deep learning-based hybrid model,” *Iran J. Comput. Sci.*, vol. 6, pp. 1–10, 2023.
- [4] M. Ali *et al.*, “Brain tumor detection and classification using PSO and convolutional neural network,” *Comput. Mater. Contin.*, vol. 73, no. 3, pp. 4501–4518, 2022.
- [5] K. Prabha, B. Nataraj, A. Karthikeyan, N. Mukilan, and M. Parkavin, “MRI imaging for the detection and diagnosis of brain tumors,” in *2023 4th Int. Conf. on Smart Electron. Commun. (ICOSEC)*, 2023, pp. 1541–1546.
- [6] L. Yuan *et al.*, “An improved method for CFNet identifying glioma cells,” in *Int. Conf. on Intell. Comput.*, 2023, pp. 97–105.
- [7] I. Decimo, G. Fumagalli, V. Berton, M. Krampera, and F. Bifari, “Meninges: From protective membrane to stem cell niche,” *Am. J. Stem Cells*, vol. 1, no. 2, pp. 92–105, 2012.
- [8] S. Bibi *et al.*, “MSRNet: Multiclass skin lesion recognition using additional residual block based fine-tuned deep models information fusion and best feature selection,” *Diagn.*, vol. 13, pp. 3063, 2023.
- [9] M. O. Khairandish, M. Sharma, V. Jain, J. M. Chatterjee, and N. Jhanjhi, “A hybrid CNN-SVM threshold segmentation approach for tumor detection and classification of MRI brain images,” *IRBM*, vol. 43, no. 4, pp. 290–299, 2022.
- [10] J. Naz *et al.*, “Recognizing gastrointestinal malignancies on WCE and CCE images by an ensemble of deep and handcrafted features with entropy and PCA based features optimization,” *Neural Process. Lett.*, vol. 55, pp. 115–140, 2023.
- [11] A. B. Menegotto and S. C. Cazella, “Multimodal deep learning for computer-aided detection and diagnosis of cancer: Theory and applications,” in *Enhanced Telemedicine and E-Health: Advanced IoT Enabled Soft Computing Framework*, Swiss, Springer, Cham, 2021, pp. 267–287.
- [12] S. Ali, J. Li, Y. Pei, R. Khurram, K. U. Rehman and T. Mahmood, “A comprehensive survey on brain tumor diagnosis using deep learning and emerging hybrid techniques with multi-modal MR image,” *Arch. Comput. Method Eng.*, vol. 29, pp. 4871–4896, 2022.
- [13] S. E. Amin and M. Megeed, “Brain tumor diagnosis systems based on artificial neural networks and segmentation using MRI,” in *2012 8th Int. Conf. Inform. Syst. (INFOS)*, 2012, pp. MM-119–MM-124.
- [14] T. Tazin *et al.*, “A robust and novel approach for brain tumor classification using convolutional neural network,” *Comput. Intell. Neurosci.*, vol. 2021, pp. 1–11, 2021.
- [15] M. K. Abd-Ellah, A. I. Awad, H. F. Hamed, and A. A. Khalaf, “Parallel deep CNN structure for glioma detection and classification via brain MRI Images,” in *2019 31st Int. Conf. on Microelectron. (ICM)*, 2019, pp. 304–307.

- [16] P. Afshar, K. N. Plataniotis, and A. Mohammadi, "Capsule networks for brain tumor classification based on MRI images and coarse tumor boundaries," in *ICASSP 2019-2019 IEEE Int. Conf. on Acoustics, Speech and Signal Process. (ICASSP)*, 2019, pp. 1368–1372.
- [17] M. Nazir, F. Wahid, and S. Ali Khan, "A simple and intelligent approach for brain MRI classification," *J. Intell. Fuzzy Syst.*, vol. 28, pp. 1127–1135, 2015.
- [18] L. Liu, H. Zhang, I. Rekik, X. Chen, Q. Wang and D. Shen, "Outcome prediction for patient with high-grade gliomas from brain functional and structural networks," in *Med. Image Comput. Comput.-Assist. Intervention–MICCAI 2016: 19th Int. Conf., Proc., Part II 19*, Athens, Greece, Oct. 17–21, 2016, pp. 26–34.
- [19] A. Sawant, M. Bhandari, R. Yadav, R. Yele, and M. S. Bendale, "Brain cancer detection from MRI: A machine learning approach (tensorflow)," *Brain*, vol. 5, pp. 2089–2094, 2018.
- [20] I. Soesanti, M. Avizenna, and I. Ardiyanto, "Classification of brain tumor MRI image using random forest algorithm and multilayers perceptron," *J. Eng. Appl. Sci.*, vol. 15, pp. 3385–3390, 2020.
- [21] M. I. Sharif, M. A. Khan, M. Alhussein, K. Aurangzeb, and M. Raza, "A decision support system for multimodal brain tumor classification using deep learning," *Complex Intell. Syst.*, vol. 8, pp. 1–14, 2021.
- [22] M. A. Khan *et al.*, "Multimodal brain tumor classification using deep learning and robust feature selection: A machine learning application for radiologists," *Diagn.*, vol. 10, no. 8, pp. 565, 2020.
- [23] A. Saleh, R. Sukaik, and S. S. Abu-Naser, "Brain tumor classification using deep learning," in *2020 Int. Conf. Assist. Rehabil. Technol. (iCareTech)*, 2020, pp. 131–136.
- [24] F. J. Díaz-Pernas, M. Martínez-Zarzuela, M. Antón-Rodríguez, and D. González-Ortega, "A deep learning approach for brain tumor classification and segmentation using a multiscale convolutional neural network," *Healthcare*, vol. 9, no. 2, pp. 153, 2021.
- [25] A. Çinar and M. Yildirim, "Detection of tumors on brain MRI images using the hybrid convolutional neural network architecture," *Med. Hypotheses*, vol. 139, pp. 109684, 2020.
- [26] A. Anil, A. Raj, H. A. Sarma, N. Chandran, and P. L. Deepa, "Brain tumor detection from brain MRI using deep learning," *Int. J. Innov. Res. Appl. Sci. Eng. (IJIRASE)*, vol. 3, pp. 458–465, 2019.
- [27] C. Jun, "Brain tumor dataset figshare," *Dataset*, 2017. doi: [10.6084/m9.figshare.1512427.v5](https://doi.org/10.6084/m9.figshare.1512427.v5).
- [28] M. A. Gómez-Guzmán *et al.*, "Classifying brain tumors on magnetic resonance imaging by using convolutional neural networks," *Electron.*, vol. 12, no. 4, pp. 955, 2023.
- [29] M. Nickparvar, "Brain tumor MRI dataset," vol. 1, 2021. doi: [10.34740/kaggle/dsv/2645886](https://doi.org/10.34740/kaggle/dsv/2645886).
- [30] S. Deepak and P. Ameer, "Brain tumor classification using deep CNN features via transfer learning," *Comput. Biol. Med.*, vol. 111, pp. 103345, 2019.
- [31] M. S. I. Khan *et al.*, "Accurate brain tumor detection using deep convolutional neural network," *Comput. Struct. Biotechnol. J.*, vol. 20, pp. 4733–4745, 2022.
- [32] N. Ghassemi, A. Shoeibi, and M. Rouhani, "Deep neural network with generative adversarial networks pre-training for brain tumor classification based on MR images," *Biomed. Signal Process.*, vol. 57, pp. 101678, 2020.
- [33] M. Masood *et al.*, "A novel deep learning method for recognition and classification of brain tumors from MRI images," *Diagn.*, vol. 11, no. 5, pp. 744, 2021.
- [34] A. M. Gab Allah, A. M. Sarhan, and N. M. Elshennawy, "Classification of brain MRI tumor images based on deep learning PGGAN augmentation," *Diagn.*, vol. 11, pp. 2343, 2021.
- [35] F. Zulfiqar, U. I. Bajwa, and Y. Mehmood, "Multi-class classification of brain tumor types from MR images using EfficientNets," *Biomed Signal Process.*, vol. 84, p. 104777, 2023.